

The role of molecular structure on impact resistance and bending strength of photocured urethane-dimethacrylate polymer networks

Izabela Barszczewska-Rybarek¹

Received: 8 August 2016/Revised: 1 February 2017/Accepted: 10 February 2017/

Published online: 16 February 2017

© The Author(s) 2017. This article is published with open access at Springerlink.com

Abstract The objective of this study was to investigate the influence of molecular structure on impact resistance (a_n) and bending strength (σ) of photocured urethane-dimethacrylate polymer networks. Urethane-dimethacrylate (UDMA) monomers were synthesized through reaction of oligoethylene glycol monomethacrylate (OEGMMA) with diisocyanate (DI). OEGMMA varied within the length of the oligooxyethylene chain, which consisted of one to four oxyethylene units. DI varied in chemical character: aliphatic, cycloaliphatic or aromatic. The molecular structure of UDMA polymers was characterized by X-ray powder diffraction, which allowed the calculation of the d -spacing (d) and dimensions of microgel agglomerates (D). The measurements of the polymerization shrinkage were used for the determination of the degree of conversion (DC), whereas the concentration of double bonds was used as a measure of the crosslink density (q). It was found that all structural parameters depend on the UDMA chemical structure. The increasing length of the oligooxyethylene chains caused the decrease in d and q , in contrast to the increase in D and DC. The DI chemical character caused the increase in the DC and q accordingly: symmetrical cycloaliphatic or aromatic < asymmetrical cycloaliphatic and aromatic < substituted aliphatic < linear aliphatic. The compact packing and high DC in polymers derived from aliphatic DIs gave rise to the decrease in d and the increase in D . The non-planar conformation of cycloaliphatic DIs emerged in high d as well as D . The planar conformation of aromatic DIs resulted in the decrease in d as well as D . The study indicated that mechanical behavior of UDMA

Electronic supplementary material The online version of this article (doi:10.1007/s00289-017-1944-z) contains supplementary material, which is available to authorized users.

✉ Izabela Barszczewska-Rybarek
Izabela.Barszczewska-Rybarek@polsl.pl

¹ Department of Physical Chemistry and Technology of Polymers, Silesian University of Technology, M. Strzody 9, 44-100 Gliwice, Poland

polymer networks can be explained in terms of the structural parameters. DC and q appeared to be the main factors determining both mechanical properties of poly(UDMA)s. The a_n was also shown to be affected by d . Particularly high linear correlations were found on a semi-logarithmic scale for the DC and d with a_n . a_n increased as the DC increased, whereas d decreased.

Keywords Urethane-dimethacrylate · Polymer networks · Nanoheterogeneity · X-ray powder diffraction · Impact resistance

Introduction

Urethane-dimethacrylate resins are a special type of monomers, which after curing combine the advantages of poly(dimethacrylate)s and polyurethanes. They undergo extensive radical crosslinking polymerization due to the presence of two double bonds in one molecule [1–9]. Through the combinations of varied monofunctional oligoethylene glycols methacrylates and varied diisocyanates in the UDMA monomer synthesis the properties of crosslinked materials can easily be tailored ranging from elastomers to thermosets [10]. The versatility of their structures results in the broad and growing spectrum of applications. They are particularly suitable for the high demands of dentistry [11], tissue engineering [12], coating and printing industries [13].

The kinetics of polymerization of tetrafunctional urethane-dimethacrylate monomers is complicated and it controls the molecular organization of the resulting polymer networks [1, 5]. If compared to the polymerization of monovinyl monomers, this process exhibits anomalous reaction behaviors, such as autoacceleration, autodeceleration, unequal functional group reactivity, reaction–diffusion controlled termination and limited functional group conversion due to hindered mobility of vinyl groups. Additionally, one of the most important characteristics of this process is the formation of highly crosslinked microgels their agglomeration into clusters and their connections in the less crosslinked matrix [1–8]. All these features lead to the formation of structural heterogeneity, which finally rules physico-mechanical behavior of urethane-dimethacrylate polymer networks.

Since poly(urethane-dimethacrylate)s are highly crosslinked infusible and insoluble polymers their structural heterogeneity is difficult to quantitatively characterize and no comprehensive methodologies have yet been established that correlate structure and morphology with ultimate properties. Techniques, such as Fourier transform infrared spectroscopy (FTIR) [3, 7, 14], solid state NMR [15], differential scanning calorimetry (DSC) [16] and measurements of the theoretical and experimental polymerization shrinkage [10] are used for the degree of conversion (DC) determination.

The degree of conversion (DC) provides information about the level of crosslinking by the double bond consumption. The literature states that the higher the conversion of double bonds, the higher the mechanical strength [2, 3, 17], modulus [2, 17], impact resistance [2, 3] and hardness [2, 18]. In addition to the DC, other factors, such as the microgel agglomerates and the strength of hydrogen bonds

are also suspected to have an influence on the mechanical performance of poly(dimethacrylate)s [2, 3, 5, 7, 9]. Dynamic mechanical analysis (DMA) [7] and thermogravimetry (TGA) [19] deliver only the general information about the structural heterogeneity, by confirming the microgel formation. However, in-depth knowledge of the molecular organization in UDMA polymer networks is still lacking. Despite the fact, that each of these methods is invaluable in studying the structure of linear polyurethanes [20, 21], they have a number of limitations, when poly(urethane-dimethacrylate)s are tested.

Recent research on dimethacrylate polymer networks identified X-ray powder diffraction (XRPD) as a promising tool for the quantitative characterization of their molecular structure [2, 3]. Although X-ray spectroscopy is an established tool for quantitative characterization of semicrystalline polymers, its quantitative application in characterizing the structure of amorphous polymeric materials is relatively new and constitutes an active area of research [2, 3, 22, 23].

The aim of this study was in assessing the suitability of XRPD for studying the molecular structure of urethane-dimethacrylate (UDMA) polymer networks to serve as an important element in the development of accurate methodology for identifying the origin of their physical and mechanical behavior.

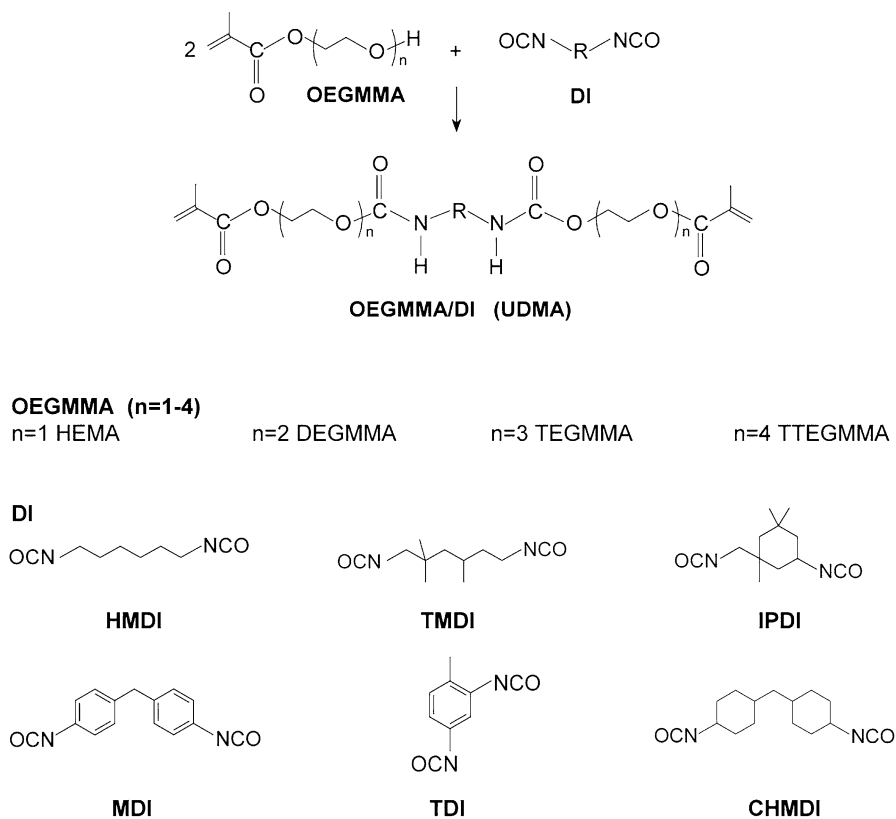
For this purpose, a family of 24 UDMA homopolymer networks was studied. Each UDMA monomer consisted of two oligoethylene glycol monomethacrylate (OEGMMA) wings, having from one to four oxyethylene units in the chain, and the core derived from one of six the most widely used diisocyanates [20, 21] (DI): aliphatic—HMDI and TMDI, cycloaliphatic—IPDI and CHMDI, aromatic—TDI and MDI (Scheme 1).

Polymer structural heterogeneity was interpreted from the perspective of the chemical structure, the degree of conversion, chemical and physical crosslink density as well as parameters possessed from XRPD experiments. The structural results were related to impact resistance and bending strength—as mechanical properties and to glass temperature—representing physico-chemical properties.

Experimental

Monomer preparation

Urethane-dimethacrylate monomers (UDMA) were synthesized from oligoethylene glycols monomethacrylates (OEGMMA) and diisocyanates (DI) according to the procedure previously reported [24, 25]. OEGMMAs: DEGMMA, TEGMMA and TTEGMMA were obtained through a trans-esterification reaction of methyl methacrylate (MMA, Acros, Geel, Belgium) with the corresponding glycols: diethylene (DEG, Acros, Geel, Belgium), triethylene (TEG, Acros, Geel, Belgium) and tetraethylene (TTEG, Acros, Geel, Belgium), according to the procedure previously reported [24, 25]. 2-Hydroxyethyl methacrylate (HEMA, Sigma-Aldrich, St. Louis, MO, USA), 1,6-hexamethylene diisocyanate (HMDI, Fluka, Taufkirchen, Germany), 2,2,4(2,4,4)-trimethylhexyl-1,6-diisocyanate (TMDI, Sigma-Aldrich, St. Louis, MO, USA), isophorone diisocyanate (IPDI, Sigma-Aldrich, St. Louis, MO,



Scheme 1 The structure of UDMA monomers

USA), 4,4'-methylenebis(cyclohexyl isocyanate) (CHMDI, Sigma-Aldrich, St. Louis, MO, USA), 2,4-toluene diisocyanate (TDI, Sigma-Aldrich, St. Louis, MO, USA) and 4,4'-methylenebis(phenyl isocyanate) (MDI, Sigma-Aldrich, St. Louis, MO, USA) were used as received.

Photocuring

The monomers were mixed with: 0.4 wt% of camphorquinone (CQ, Sigma-Aldrich, St. Louis, MO, USA)—the photosensitizer, and 1 wt% of *N,N*-dimethylaminoethyl methacrylate (DMAEMA, Sigma-Aldrich, St. Louis, MO, USA)—the reducing agent, and poured into moulds. Petri dishes (120 mm in diameter and 4-mm thick) were used for this purpose. The samples were covered with PET film to reduce the oxygen inhibition effect and then irradiated for 30 min. Photopolymerization was initiated with a high pressure mercury vapor lamp (FAMED-1, model L-6/58, Lodz, Poland, power 375 W, emitting UV/VIS light). This procedure has been developed and tested for the purposes of previous works [2, 10].

Table 1 Thermal properties of UDMA monomers and temperatures of their polymerization [14]

OEGMMA	$T_m/T_p/T_o$ (°C)					
	HMDI	TMDI	IPDI	CHMDI	TDI	MDI
$n = 1$ HEMA	77/91/155	RT _p	RT _p	108/125/195	98/114/181	89/103/161
$n = 2$ DEGMMA	RT _p	RT _p	RT _p	RT _p	RT _p	RT _p
$n = 3$ TEGMMA	RT _p	RT _p	RT _p	RT _p	RT _p	RT _p
$n = 4$ TTEGMMA	RT _p	RT _p	RT _p	RT _p	RT _p	RT _p

T_m melting temperature of the monomer

T_p temperature at which the photopolymerization was carried out

T_o onset of the temperature of thermal polymerization

RT_p room temperature, at which liquid monomers were photopolymerized

The photopolymerization of liquid monomers was performed at room temperature. Solid monomers (HEMA/HMDI, HEMA/CHMDI, HEMA/TDI and HEMA/MDI) were mixed with the initiation system, introduced into moulds and photopolymerized in the molten state. Before irradiation, each monomer was fused at a temperature lower than the temperature of its thermal polymerization, as found in DSC experiments [14]. The detailed information about polymerization conditions are provided in Table 1.

Degree of conversion and crosslink density

The monomer density (d_m) was measured utilizing a liquid pycnometer at 25 °C according to ISO 1675 (Plastics—liquid resins—determination of density by the pycnometer method). The polymer density (d_p) was determined according to the Archimedes' principle, on the Mettler Toledo XP Balance with 0.01 mg accuracy (Greifensee, Switzerland) with the density determination kit at 25 °C. Water was used as the immersing liquid. The volumetric shrinkage of photopolymerized samples was determined by the following equations:

$$S_e = \frac{d_p - d_m}{d_p}, \quad (1)$$

$$S_t = \frac{d_m \times 2 \times 22.5}{MW}, \quad (2)$$

where S_e is the experimentally determined polymerization shrinkage, S_t is the polymerization shrinkage extrapolated to the full conversion [8] and MW is a monomer molecular weight.

The degree of conversion (DC) was calculated according to the following formula:

$$DC = \frac{S_e}{S_t}. \quad (3)$$

The crosslink density (q) was calculated using the following equation:

$$q = X_{\text{DB}} \times \text{DC}, \quad (4)$$

where X_{DB} is the concentration of double bonds in the UDMA monomer.

Glass transition temperature

The glass transition temperature (T_g) values were taken from the previous studies [10, 24, 25]. The rectangular samples of polymers (length \times width \times thickness: 50 mm \times 5 mm \times 2 mm) were examined using dynamic mechanical analysis (Polymer Laboratories MK II DMA apparatus, Shropshire, UK). Experiments were performed in bending mode and a frequency of 1 Hz. The T_g was taken as the temperature at the tan delta peak maximum.

X-ray powder diffraction (XRPD)

XRPD experiments were carried out using Siemens D 5005 X-ray powder diffractometer (Berlin, Germany) employing filtered Cu K α radiation. The powdered samples of all polymers, having the particle size of less than 100 μm were analyzed.

The relative peak intensity (I) was calculated according to the equation:

$$I(\%) = \frac{I_2}{I_1} \times 100, \quad (5)$$

where I_2 is intensity of the less intense peak, I_1 is the intensity of the more intense peak.

The d -spacing (d) was calculated using Bragg's equation:

$$d(\text{\AA}) = \frac{\lambda}{2 \sin \theta} \quad (6)$$

where λ is the wavelength of the radiation ($\lambda = 1.54184 \text{ \AA}$), θ is the Bragg angle.

The particle size (D) was calculated using the Scherrer's equation:

$$D(\text{nm}) = \frac{k\lambda}{\beta_D \cos \theta} \quad (7)$$

where k is the constant ($k = 1$), β_D is the peak width taken as the full width at half maximum intensity.

Mechanical testing

The four point bending tests were performed according to DIN 53435 (Testing of plastics, bending test and impact test on dynstat test pieces) using VEB Werkstoffprüfmaschinen dynstat apparatus. Test bar samples of 10-mm width and 15-mm length were cut from moulds of 4-mm thick, prepared in the above

mentioned procedure of curing. The bending strength (σ) and the impact strength (a_n) were calculated, respectively, from the following equations:

$$\sigma(\text{MPa}) = \frac{6M_c}{bh^2}, \quad (8)$$

$$a_n(\text{kJ/m}^2) = \frac{A_n}{bh}, \quad (9)$$

where M_c is the bending moment, A_n is the impact energy causing a material fracture, b is the sample width and h is the sample thickness.

Results

The monomer/polymer chemical structure

In this work, a series of urethane dimethacrylate (UDMA) monomers were synthesized [24, 25] and then homopolymerized according to the procedures previously described in the literature [2, 9, 10, 14]. The monomer chemical structure was confirmed by ^1H NMR analysis (Supporting information, Figures S1–S6). The polymer formation was confirmed by FTIR analysis (Supporting Information, Figure S7). In an effort to understand the structure–property relationships in polymer networks, the UDMA chemical structure was modified by extending the OEGMMA wings and the use of different DI core. For this purpose, four OEGMMAs, having from one to four oxyethylene groups in the chain, and six DIs: HMDI and TMDI (aliphatic), CHMDI and IPDI (cycloaliphatic) as well as TDI and MDI (aromatic) were used in the syntheses of monomers (Scheme 1). These structural diversifications provided the range of monomer molecular weights (MW), concentrations of double bonds (X_{DB}) as well as urethane bonds (X_{UB}) (Table 2). The monomers were homopolymerized in the UV/VIS light-induced process, using the camphorquinone/tertiary amine photo-initiating system, under identical conditions.

The polymer network molecular structure

The molecular structure of UDMA polymer networks was characterized by the degree of conversion (DC), which was determined by measuring the experimental (S_e) and the theoretical polymerization shrinkages (S_t). As shown in Table 2, the DC increased as the oligooxyethylene chain length increased. The DI also affected the DC, which decreased in the following order: HMDI > TMDI > IPDI \approx TDI > CHMDI \approx MDI. Generally, fully aliphatic UDMA polymerized to higher DC than those having cycloaliphatic and aromatic moieties. Polymers produced from linear OEGMMA/HMDI homologous series had the highest DC. In comparison, multiple methyl substitution in TMDI caused a drop in the DC. UDMA having symmetrically substituted rings (CHMDI and MDI) polymerized to a lower DC than those possessing asymmetrically substituted rings (IPDI and TDI).

Table 2 The properties of studied UDMA monomers: molecular weight (MW), concentration of double bonds (X_{DB}), concentration of urethane bonds (X_{UB}) and the corresponding polymers: degree of conversion (DC) [10], crosslink density (q)

Monomer	MW (g/mol)	X_{DB}/X_{UB} (mol/kg)	DC	q
HEMA/HMDI	428.5	4.67	0.70 (0.05)	3.28 (0.21)
DEGMMA/HMDI	516.6	3.87	0.79 (0.06)	3.05 (0.25)
TEGMMA/HMDI	604.7	3.31	0.83 (0.06)	2.76 (0.21)
TTEGMMA/HMDI	692.8	2.89	0.74 (0.06)	2.13 (0.18)
HEMA/TMDI	470.6	4.25	0.65 (0.04)	2.78 (0.18)
DEGMMA/TMDI	558.7	3.58	0.75 (0.05)	2.67 (0.18)
TEGMMA/TMDI	646.8	3.09	0.78 (0.04)	2.40 (0.11)
TTEGMMA/TMDI	735.0	2.72	0.85 (0.05)	2.30 (0.14)
HEMA/IPDI	482.5	4.15	0.52 (0.04)	2.14 (0.17)
DEGMMA/IPDI	570.7	3.50	0.57 (0.06)	1.98 (0.21)
TEGMMA/IPDI	658.8	3.04	0.61 (0.07)	1.86 (0.21)
TTEGMMA/IPDI	746.9	2.68	0.69 (0.05)	1.84 (0.14)
HEMA/CHMDI	522.7	3.83	0.46 (0.06)	1.74 (0.24)
DEGMMA/CHMDI	610.8	3.27	0.51 (0.07)	1.67 (0.24)
TEGMMA/CHMDI	698.9	2.86	0.58 (0.07)	1.67 (0.21)
TTEGMMA/CHMDI	787.0	2.54	0.64 (0.06)	1.61 (0.15)
HEMA/TDI	434.4	4.60	0.52 (0.05)	2.41 (0.22)
DEGMMA/TDI	522.6	3.83	0.53 (0.06)	2.02 (0.19)
TEGMMA/TDI	610.7	3.27	0.59 (0.06)	1.92 (0.19)
TTEGMMA/TDI	698.8	2.86	0.63 (0.06)	1.80 (0.16)
HEMA/MDI	510.6	3.92	0.46 (0.05)	1.79 (0.18)
DEGMMA/MDI	598.7	3.34	0.47 (0.05)	1.56 (0.15)
TEGMMA/MDI	686.8	2.91	0.54 (0.08)	1.56 (0.22)
TTEGMMA/MDI	774.9	2.58	0.55 (0.07)	1.42 (0.19)

In this study, the concentration of double bonds (X_{DB}) was used as a measure of the theoretical crosslink density. X_{DB} was calculated from the monomer molecular weight for each UDMA monomer (Table 2). As each UDMA has two urethane bonds as well as two double bonds, the crosslink density resulting from the presence of physical crosslinking (X_{UB}) was also calculated. X_{UB} adopted the same values as X_{DB} . UDMA with higher MW were characterized by lower X_{DB} (X_{UB}) values, and therefore they were expected to form networks of lower crosslink density. X_{DB} (X_{UB}) decreased as the OEGMMA length increased and the DI altered in the following order: HMDI > TDI > TMDI > IPDI > MDI > CHMDI.

Having the DC values, X_{DB} was reduced by the fraction of unreacted double bonds and the obtained values were treated as a measure of the real crosslink density (q) (Table 2). The values of q decreased as the OEGMMA length increased and as the DI altered in the following order: HMDI > TMDI > TDI > IPDI > CHMDI > MDI.

The XRPD quantitative analysis of the polymer network structural heterogeneity

As representatively shown in Fig. 1, the diffractograms of studied poly(UDMA)s consisted of two broad diffuse peaks. The stronger peak was located at around 2θ value of 19.4° , whereas the weaker one was located at around 43.3° . The differences in the peak intensity, position and broadening were observed along with the UDMA diversification. Therefore, the relationships between polymer chemical structure and morphological features were examined by classifying results according to the peak intensity (I), d -spacing (d) and particle size (D) (Table 3).

The peak relative intensity changed with the UDMA chemical structure. Primarily, with the lengthening of the oligooxyethylene chain the stronger peak gained intensity (I_1), whereas the weaker peak lost intensity (I_2), which caused decreases in I within particular homologous series. Exceptionally, poly(HEMA/IPDI) and poly(HEMA/CHMDI) were characterized by I lower than their DEGMMA-based homologous. According to the DI, the following decreasing trend of mean I values can be constructed: IPDI > TDI > MDI > TMDI > CHMDI > HMDI.

The presence of two peaks in the XRPD patterns suggests the detection in the experiments two average distances between diffracting planes (d). The stronger peak, positioned at lower 2θ values, corresponded to larger d -spacing than the peak, located at higher 2θ values. The d_1 values ranged from 4.09 to 4.95 nm, whereas the average d_2 value equaled to 2.1 nm. With the increasing OEGMMA length the stronger peak shifted to higher diffraction angles, whereas the weaker peak remained unmoved. Consequently, the average drop of d_1 within a homologous series was of 7% (Table 3).

The influence of the DI on d_1 was also seen (Table 3). The mean values of d_1 increased in the following order: HMDI \approx TDI \approx MDI < TMDI < IPDI \approx CHMDI. As can be seen from Table 3, similar d_1 values were identified

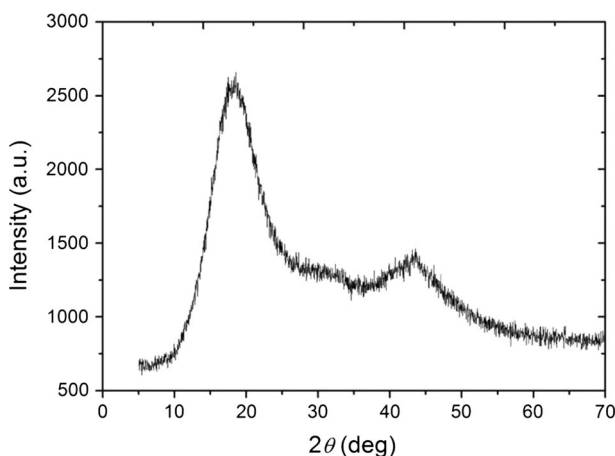


Fig. 1 The exemplary XRPD diffractogram of HEMA/TMDI polymer network

Table 3 The XRPD parameters obtained for UDMA polymer networks: the relative peak intensity (I), the peak position (2θ), the d -spacing (d), the particle dimension (D)

UDMA polymer networks	I (%)	$2\theta_1$ (°)	d_1 (Å)	$2\theta_2$ (°)	d_2 (Å)	D_1 (nm)	D_2 (nm)
HEMA/HMDI	28.9 (1.2)	19.49 (1.61)	4.56 (0.27)	43.39 (1.72)	2.09 (0.06)	2.08 (0.22)	1.38 (0.33)
DEGMMMA/HMDI	26.7 (1.8)	19.68 (1.56)	4.51 (0.30)	43.45 (1.94)	2.08 (0.06)	2.09 (0.19)	1.51 (0.41)
TEGMMMA/HMDI	22.1 (2.2)	20.51 (2.24)	4.33 (0.34)	43.05 (1.85)	2.10 (0.06)	2.19 (0.19)	1.33 (0.40)
TTEGMMMA/HMDI	20.4 (1.4)	21.70 (1.55)	4.09 (0.23)	42.82 (1.77)	2.11 (0.06)	2.15 (0.19)	1.31 (0.37)
HEMA/TMDI	32.1 (1.5)	18.08 (1.35)	4.91 (0.25)	43.33 (1.81)	2.09 (0.06)	2.06 (0.17)	1.87 (0.35)
DEGMMMA/TMDI	27.9 (1.7)	18.64 (1.27)	4.76 (0.25)	43.36 (1.84)	2.09 (0.06)	2.04 (0.18)	1.35 (0.47)
TEGMMMA/TMDI	25.1 (2.5)	19.36 (1.23)	4.59 (0.27)	43.33 (1.88)	2.09 (0.06)	2.07 (0.23)	1.60 (0.29)
TTEGMMMA/TMDI	23.6 (1.9)	19.47 (1.55)	4.56 (0.27)	43.24 (1.69)	2.09 (0.05)	2.06 (0.19)	1.50 (0.45)
HEMA/IPDI	31.0 (2.2)	17.91 (1.94)	4.95 (0.32)	43.42 (1.90)	2.08 (0.06)	1.91 (0.17)	1.67 (0.39)
DEGMMMA/IPDI	37.2 (2.0)	18.12 (1.25)	4.89 (0.31)	43.63 (1.82)	2.08 (0.06)	1.94 (0.20)	1.72 (0.46)
TEGMMMA/IPDI	29.9 (1.9)	19.17 (1.29)	4.63 (0.27)	43.43 (1.91)	2.08 (0.06)	1.95 (0.16)	1.67 (0.51)
TTEGMMMA/IPDI	26.2 (1.9)	19.50 (1.53)	4.55 (0.27)	43.36 (1.87)	2.09 (0.06)	1.90 (0.16)	1.88 (0.55)
HEMA/CHMDI	24.5 (2.1)	17.99 (1.57)	4.93 (0.23)	43.27 (1.79)	2.09 (0.06)	2.14 (0.20)	1.68 (0.48)
DEGMMMA/CHMDI	27.2 (1.9)	18.51 (1.52)	4.79 (0.25)	43.17 (1.74)	2.10 (0.06)	2.16 (0.22)	1.33 (0.38)
TEGMMMA/CHMDI	24.3 (2.2)	19.11 (1.50)	4.64 (0.26)	43.06 (1.80)	2.10 (0.06)	2.16 (0.20)	1.63 (0.26)
TTEGMMMA/CHMDI	21.8 (1.6)	19.65 (1.51)	4.52 (0.25)	42.99 (1.85)	2.10 (0.06)	2.18 (0.18)	1.45 (0.50)
HEMA/TDI	33.9 (2.3)	19.60 (1.41)	4.53 (0.22)	43.33 (1.97)	2.09 (0.06)	1.38 (0.15)	1.26 (0.36)
DEGMMMA/TDI	30.4 (1.7)	20.14 (1.56)	4.41 (0.27)	43.44 (1.83)	2.08 (0.06)	1.46 (0.20)	1.14 (0.26)
TEGMMMA/TDI	27.5 (2.0)	20.43 (1.76)	4.35 (0.29)	43.28 (1.78)	2.09 (0.06)	1.66 (0.19)	1.28 (0.29)
TTEGMMMA/TDI	24.6 (2.3)	20.49 (2.02)	4.33 (0.27)	43.23 (1.80)	2.09 (0.06)	1.83 (0.20)	1.35 (0.26)
HEMA/MDI	29.1 (1.9)	19.53 (1.52)	4.54 (0.29)	43.76 (1.71)	2.07 (0.05)	1.63 (0.18)	1.26 (0.39)
DEGMMMA/MDI	28.0 (2.2)	19.65 (1.28)	4.52 (0.25)	43.81 (1.90)	2.07 (0.06)	1.58 (0.19)	1.11 (0.21)
TEGMMMA/MDI	27.0 (2.4)	20.29 (1.91)	4.38 (0.34)	43.69 (1.88)	2.07 (0.06)	1.72 (0.15)	1.21 (0.38)
TTEGMMMA/MDI	25.6 (2.2)	20.70 (1.44)	4.29 (0.22)	43.53 (1.78)	2.08 (0.06)	1.87 (0.18)	1.28 (0.31)

Subscript 1 refers to the stronger peak at around 19.4° of 2θ and appendix 2 refers to the weaker peak at around 43.4° of 2θ . Brackets show standard deviations of five tests

for polymer networks having HMDI, TDI and MDI moieties, and they were lower than d_1 values of polymer networks having TMDI, IPDI and CHMDI moieties. When comparing only fully aliphatic polymers, the average d -spacing of those having the linear HMDI structure was smaller than the average d -spacing of polymers having multi-methyl-substituted TMDI. Poly(UDMA)s with aromatic rings were characterized by smaller d -spacing than polymers with cycloaliphatic rings.

Since each peak in the diffractogram can be interpreted with varied dimensions of ordered domains, the D_1 and D_2 structural parameters were calculated (Table 3). D_1 corresponds to the better resolved peak, located at lower diffraction angles and its values ranged from 1.38 to 2.19 nm. The values of D_2 ranged from 1.11 to 1.87 nm; however, due to the lower peak resolution they had higher experimental error. The results for D_1 and D_2 showed that polymers having aromatic rings organize into smaller agglomerates than the remaining UDMA.s.

The glass transition

The T_g of UDMA polymers ranged from -10 to 194 °C and decreased with the lengthening of OEGMMA, as shown in Table 4. The T_g was also influenced by the DI and its values increased in the following general order: HMDI < TMDI < IPDI \approx TDI \approx MDI < CHMDI. The fully aliphatic networks had significantly lower T_g than polymers starting from the remaining DIs. The symmetry in the aromatic and cycloaliphatic DIs (MDI and CHMDI) resulted in the increase in the polymer T_g if compared to the influence of the asymmetrical DIs (TDI and IPDI) on the T_g of polymers.

Mechanical properties

As can be seen in Table 4, bending strength of UDMA polymer networks depends on the OEGMMA and DI. Its values increased when the length of the OEGMMA increased. Polymers consisting of TTEGMMA did not break in bending tests as well as fully aliphatic polymers consisting of TEGMMA. When comparing polymers by the DI, the following increasing order of σ can be constructed: MDI < TDI < IPDI = CHMDI < TMDI < HMDI.

In Table 4 the impact strength values are also summarized. It can be seen that the impact strength of UDMA polymer networks increased as the OEGMMA was lengthened. Additionally, logarithmic correlations were found between the impact resistance and the DC, q as well as d_1 . R^2 was calculated separately for a particular homologous series of polymer networks. Its average values equaled 0.953, 0.910 and 0.947 (Table 5; Fig. 2), respectively, to correlations of a_n with DC, q and d_1 . When the DI was varied, the increasing order of mean values of impact resistance was found: MDI \approx CHMDI < TDI \approx IPDI < TMDI < HMDI. Generally, there were no differences between results for polymers of CHMDI and MDI homologous series as well as IPDI and TDI.

Table 4 Mechanical and thermal properties of studied polymer networks: flexural strength (σ), impact resistance (a_n) and glass temperature (T_g)

Polymer	σ (MPa)	a_n (kJ/m ²)	T_g (°C)
HEMA/HMDI	130.5 (10.8)	3.80 (0.35)	139 ^c
DEGMMA/HMDI	151.7 (11.2)	8.26 (0.63)	67 ^c
TEGMMA/HMDI	— ^a	16.12 (1.13)	33 ^c
TTEGMMA/HMDI	— ^a	— ^b	—10 ^c
HEMA/TMDI	119.8 (10.6)	4.85 (0.50)	148 ^c
DEGMMA/TMDI	145.5 (11.1)	6.71 (0.62)	62 ^c
TEGMMA/TMDI	— ^a	11.07 (0.49)	40 ^c
TTEGMMA/TMDI	— ^a	15.19 (0.80)	20 ^c
HEMA/IPDI	93.7 (7.7)	3.12 (0.31)	194 ^c
DEGMMA/IPDI	142.2 (9.9)	4.74 (0.44)	105 ^c
TEGMMA/IPDI	157.3 (8.1)	8.83 (0.41)	83 ^c
TTEGMMA/IPDI	— ^a	14.04 (0.79)	42 ^c
HEMA/CHMDI	91.2 (11.5)	2.16 (0.30)	186 ^d
DEGMMA/CHMDI	140.5 (9.1)	3.55 (0.34)	129 ^d
TEGMMA/CHMDI	152.9 (9.6)	6.51 (0.54)	80 ^d
TTEGMMA/CHMDI	— ^a	11.30 (0.67)	71 ^d
HEMA/TDI	81.1 (9.7)	3.63 (0.39)	192 ^c
DEGMMA/TDI	134.5 (8.3)	5.64 (0.24)	111 ^c
TEGMMA/TDI	145.9 (9.0)	8.92 (0.60)	65 ^c
TTEGMMA/TDI	— ^a	12.01 (0.94)	33 ^c
HEMA/MDI	79.3 (9.9)	2.79 (0.32)	165 ^c
DEGMMA/MDI	113.1 (7.6)	3.73 (0.32)	109 ^c
TEGMMA/MDI	140.0 (5.7)	6.52 (0.41)	75 ^c
TTEGMMA/MDI	— ^a	10.81 (0.78)	46 ^c

Brackets show standard deviations of five tests

^a The polymer did not break in bending tests

^b The polymer did not break in impact tests

^c As cited in the Ref. [24]

^d As cited in the Ref. [10]

^e As cited in the Ref. [25]

Table 5 The correlation coefficients for linear functions on a semi-logarithmic scale between impact resistance and degree of conversion [$\ln a_n = f(\text{DC})$], crosslink density [$\ln a_n = f(q)$] as well as d -spacing [$\ln a_n = f(d_1)$] for a particular homologous series of UDMA polymer networks

UDMA	R^2		
	$\ln a_n = f(\text{DC})$	$\ln a_n = f(q)$	$\ln a_n = f(d_1)$
HMDI	0.98	0.988	0.861
TMDI	0.932	0.99	0.953
IPDI	0.98	0.902	0.962
CHMDI	0.999	0.876	0.998
TDI	0.892	0.914	0.923
MDI	0.939	0.789	0.985
Mean value	0.953	0.91	0.947

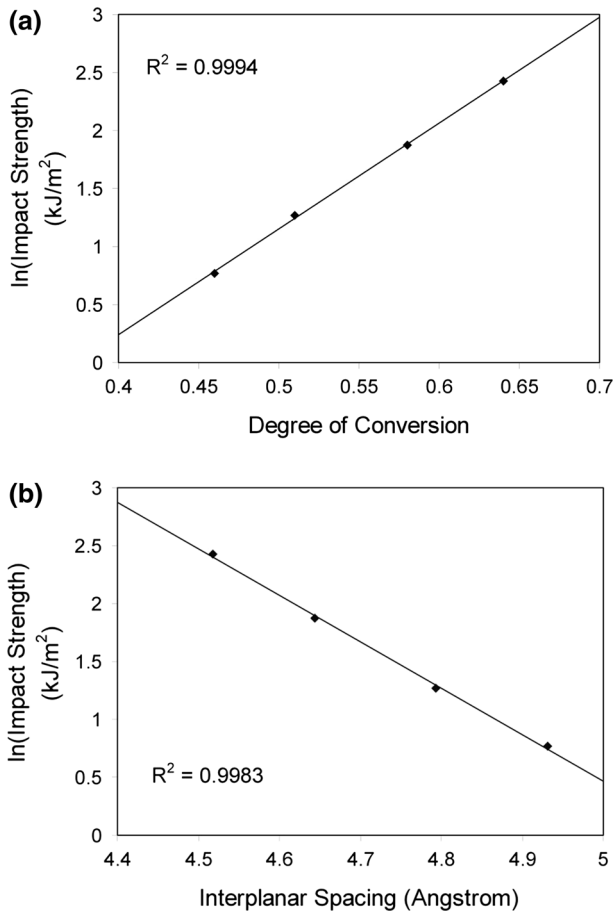


Fig. 2 The exemplary relationships on the semi-logarithmic scale between the impact resistance and: **a** the degree of conversion and **b** the interplanar spacing for polymer networks of OEGMMA/CHMDI homologous series

Discussion

The main purpose of this work was to explain basic mechanical properties of 24 urethane-dimethacrylate polymer networks through the comprehensive analysis of their molecular structure. The degree of conversion, crosslink density and the structural parameters determined by XRPD experiments were explained in terms of the monomer chemical structure and then related to glass temperature, bending strength and impact resistance.

The increase in the DC with the increasing UDMA length (Table 2) is most probably caused by the increasing mobility of pendant double bonds and decreasing limitations of the reaction diffusion. Features of the DI chemical structure, such as the aliphatic, cycloaliphatic or aromatic chemical character, presence of substituents and substitution symmetry played a further role. The fully aliphatic and linear

UDMAs polymerized to the highest DC. Particularly, the highest flexibility of HMDI-based monomers allows for a number of rotational conformations, compact packing and close proximity of reactive groups, which led to the largest polymerization extent. In comparison, multiple methyl substitution in TMDI provides steric hindrance and limits conformational changes, which caused a drop in the DC. DIs constructed of symmetrically substituted rings connected by a methylene bridge: CHMDI and MDI, are responsible for the steric hindrance, methacrylate group separation, increase of molecular stiffness. Therefore, polymers based on them had the lowest DC. The IPDI and TDI cores, due to a steric hindrance resulting from the bulkiness of the methyl-substituted rings, still limit conformational freedom. However, closer proximity of reactive groups in this case facilitated the reaction diffusion, which probably led to a moderate DC.

The evaluation of the crosslink density in poly(dimethacrylate)s was a more complicated issue. Such polymer networks, assuming they are ideal, consist of poly(methyl methacrylate) primary chains and long, spacious crosslinks, making-up the rest of the monomer molecules. These crosslinks, due to their significantly higher molecular weight compared to the methacrylate group, might be treated as the chains between two trifunctional junction points [25–27]. The difference in length between these two types of chains is so meaningful that the molecular weight of the primary chain may even be omitted in some structure–property considerations [26]. In that case, the concentration of double bonds (X_{DB}) can be used as a measurement of the theoretical crosslink density, as it was done in this study. Additionally, having the DC and X_{DB} values, the real crosslink density (q) was determined (Table 2). In contrast to the DC, q decreased with the increasing OEGMMA length. From the point of view of the DI, the DC as well q increased according to the same orders: symmetrical cycloaliphatic or aromatic < asymmetrical cycloaliphatic and aromatic < substituted aliphatic < linear aliphatic.

Another aspect of the UDMA polymer network structure to consider relates to its physical crosslinking. UDMA monomers may form strong hydrogen bonds between one of two imino proton donors and its imino, ester or ether acceptors (NH...N or NH...O). The concentration of urethane bonds (X_{UB}) was proposed as a measure of the crosslink density resulting from the presence of physical crosslinking (Table 2). By comparing the results for the physical crosslinking with q , only the order constructed from the DI perspective differed with respect to the positioning of TDI. Polymers based on TDI had the second highest X_{UB} values, which suggest that physical crosslink density of this polymer series is also the second highest.

The additional data on the molecular structure of UDMA polymer networks was obtained from XRPD experiments. Parameters, such as the relative peak intensity (I), d -spacing (d) and particle size (D) differed with the OEGMMA length and the DI chemical structure (Table 3).

The increasing contribution of linear aliphatic structural elements—the increasing number of oxyethylene units and the HMDI presence—caused the most demonstrative variations in the arrangement of ordered components and allowed for a more compact packing of the UDMA molecule. This was reflected in the decrease in I as well as d_1 and in the increase in D_1 .

When comparing the d_1 of only fully aliphatic polymers, those having the linear HMDI structure were characterized by smaller d -spacings than polymers having multi-methyl-substituted TMDI, which may be explained by chain distancing in the latter case. Another conclusion applies to the comparison of d -spacing values in polymer networks with aromatic and cycloaliphatic structures. Poly(UDMA)s with aromatic rings indicated smaller d -spacings than polymers with cycloaliphatic rings. Most probably, the planar geometry of benzene rings, present in TDI and MDI, which is less spacious than the non-planar, chair cyclohexylene conformation, present in IPDI and CHMDI, allows for building tighter structure in polymers having aromatic moieties.

The results for D_1 should be explained individually for fully aliphatic poly(UDMA)s and for those having ring DIs. Close proximity of double bonds and high level of elasticity in HMDI and TMDI-based structures led to the highest DC, q and cluster agglomeration, which reflected in the highest D_1 . On the other hand, D_1 values of polymers having cycloaliphatic and aromatic structures can be compared. Since the polymers consisted of IPDI and TDI as well as CHMDI and MDI had similar DC and q , the explanation of differences in D_1 should be sought in differences in the occupied space. Cycloaliphatic IPDI and CHMDI non-planar structures occupy more space than aromatic planar TDI and MDI structures, which reflected in lower D_1 values of polymer networks, being the homologous of the latter couple.

The results of the structural analysis were used for the interpretation of the glass transition temperature and mechanical properties of UDMA polymer networks. The length of the oligooxyethylene unit appeared to be the main factor determining glass temperature, bending strength and impact resistance of UDMA polymer networks. T_g decreased whereas σ and a_n increased as the OEGMMA was lengthened. As presented above, the lengthening of the OEGMMA causes the increase in the DC, whereas the decrease in q and d -spacing. Semi-logarithmic linear correlations (Table 5; Fig. 2) pointed out that the OEGMMA length controls the DC, q and d -spacing and these parameters in turn determine impact resistance.

The comparison of structural parameters with mechanical properties and glass temperature from the DI perspective resulted in finding that the patterns of the DC, q , a_n and T_g overlapped. The values of these parameters increased accordingly: symmetrical cycloaliphatic or aromatic < asymmetrical cycloaliphatic and aromatic < substituted aliphatic < linear aliphatic. It suggests that a_n and T_g are more sensitive to the high double bond conversion and high crosslink density than to the network tightness resulting from the d -spacing or dimensions of microgel agglomerates. Additionally, it was found that the natural logarithm of impact resistance decreases linearly with the elevation of glass temperature (Fig. 3). It confirms that T_g is governed by the same structural mechanisms as a_n ; the degree of conversion and crosslink density.

The DI caused the increase in bending strength according to a slightly different order: aromatic < cycloaliphatic < aliphatic. It means that the presence of the cycloaliphatic moiety promotes bending strength of poly(UDMA)s. It may even come at the expense of the reduced DC and q , as took place in the case of the CHMDI polymer series.

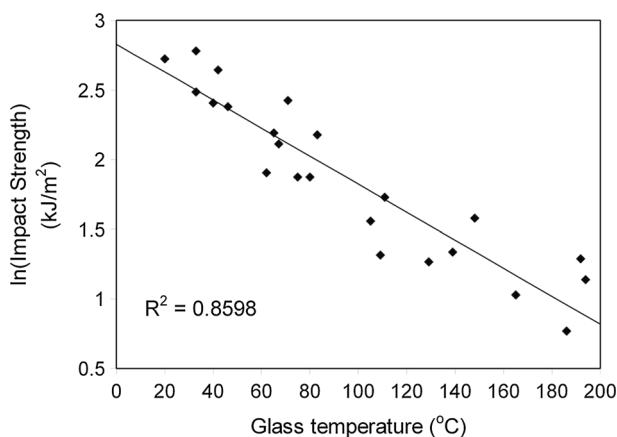


Fig. 3 The relationship on the semi-logarithmic scale between the impact resistance and the glass temperature

Conclusions

The XRPD may serve as a valuable tool in studying the molecular structure of urethane-dimethacrylate polymer networks. Parameters, such as the peak relative intensity, d -spacing and dimensions of microgel agglomerates are sensitive to the UDMA structure and vary with the lengthening of the OEGMMA wings and the alteration of the DI core.

The comprehensive analysis of X-ray parameters, the degree of conversion and crosslink density allow for the detailed quantitative characterization of structural heterogeneity of UDMA polymer networks, and in the consequence, for the explanation of their physico-mechanical properties.

The d -spacing, microgel agglomerate dimensions and degree of conversion depend on the aliphatic fraction. The increasing length of the oligooxyethylene chains causes the decrease in d and q , whereas the increase in D and DC. The presence of the moieties derived from the aliphatic DIs has the same general effect, except q , which is the highest in fully aliphatic poly(UDMA)s. The presence of the cycloaliphatic moieties, having non-planar conformation, gives rise to the increase in the d -spacing and microgel sizes. The planar conformation of aromatic rings results in the decrease in the d -spacing and microgel dimensions. The presence of asymmetrically substituted ring DIs causes the increase in the DC and q , if compared to the effect of symmetrically substituted ring DIs.

Bending strength, impact resistance and glass temperature of UDMA polymer networks increase as the DC increases. Along with the decrease in q , both mechanical properties increase, whereas T_g decreases. Additionally, impact resistance increases as the d -spacing decreases with the increase of the aliphatic fraction. Particularly high linear correlations between a_n and the DC as well as the d -spacing can be found on a semi-logarithmic scale for each homologous series of UDMA polymer networks.

Open Access This article is distributed under the terms of the Creative Commons Attribution 4.0 International License (<http://creativecommons.org/licenses/by/4.0/>), which permits unrestricted use, distribution, and reproduction in any medium, provided you give appropriate credit to the original author(s) and the source, provide a link to the Creative Commons license, and indicate if changes were made.

References

1. Andrzejewska E (2001) Photopolymerization kinetics of multifunctional monomers. *Prog Polym Sci* 26(4):605–665
2. Barszczewska-Rybarek IM (2009) Structure–property relationships in dimethacrylate networks based on Bis-GMA, UDMA and TEGDMA. *Dent Mater* 25(9):1082–1089. doi:[10.1016/j.dental.2009.01.106](https://doi.org/10.1016/j.dental.2009.01.106)
3. Barszczewska-Rybarek IM (2013) A new approach to morphology studies on diacrylate polymer networks using X-ray powder diffraction. *Macromol Chem Phys* 214(9):1019–1026. doi:[10.1002/macp.201200676](https://doi.org/10.1002/macp.201200676)
4. Di Lorenzo F, Seiffert S (2015) Nanostructural heterogeneity in polymer networks and gels. *Polym Chem* 6:5515–5528. doi:[10.1039/c4py01677g](https://doi.org/10.1039/c4py01677g)
5. Dickens SH, Stansbury JW, Choi KM, Floyd CJE (2003) Photopolymerization kinetics of methacrylate dental resins. *Macromolecules* 36:6043–6053
6. Krzeminski M, Molinari M, Defoort B, Coqueret X (2013) Nanoscale heterogeneities in radiation-cured diacrylate networks: weakness or asset? *Radiat Phys Chem* 84:79–84. doi:[10.1016/j.radphyschem.2012.06.040](https://doi.org/10.1016/j.radphyschem.2012.06.040)
7. Rey L, Duchet J, Galy J, Sautereau H, Vouagner D, Carrion L (2002) Structural heterogeneities and mechanical properties of vinyl/dimethacrylate networks synthesized by thermal free radical polymerization. *Polymer* 43(16):4375–4384. doi:[10.1016/S0032-3861\(02\)00266-5](https://doi.org/10.1016/S0032-3861(02)00266-5)
8. Szczepanski RC, Pfeifer CS, Stansbury JW (2012) A new approach to network heterogeneity: polymerization induced phase separation in photo-initiated, free-radical methacrylic systems. *Polymer* 53:4694–4701. doi:[10.1016/j.polymer.2012.08.010](https://doi.org/10.1016/j.polymer.2012.08.010)
9. Barszczewska-Rybarek IM, Jurczyk S (2015) Comparative study of structure-property relationships in polymer networks based on Bis-GMA, TEGDMA and various urethane-dimethacrylates. *Materials* 8(3):1230–1248. doi:[10.3390/ma8031230](https://doi.org/10.3390/ma8031230)
10. Barszczewska-Rybarek IM (2014) Characterization of urethane-dimethacrylate derivatives as alternative monomers for the restorative composite matrix. *Dent Mater* 30(12):1336–1344. doi:[10.1016/j.dental.2014.09.008](https://doi.org/10.1016/j.dental.2014.09.008)
11. Leprince JG, Palin WM, Hadis MA, Devaux J, Leloup G (2013) Progress in dimethacrylate-based dental composite technology and curing efficiency. *Dent Mater* 29:139–156. doi:[10.1016/j.dental.2012.11.005](https://doi.org/10.1016/j.dental.2012.11.005)
12. Park BJ, Park K, Ahn KD, Chin YO, Han DK (2006) Preparation of new bioactive hybrid bone cements containing Bis-GMA derivatives as a prepolymer. *Macromol Mater Eng* 291(6):684–689. doi:[10.1002/mame.200500408](https://doi.org/10.1002/mame.200500408)
13. Kumar V, Bhardwaj YK, Sabharwal S (2006) Coating characteristics of electron beam cured bisphenol A diglycidyl ether diacrylate resin containing 1,6-hexanediol diacrylate on wood surface. *Prog Org Coat* 55:316–323. doi:[10.1016/j.porgcoat.2006.01.002](https://doi.org/10.1016/j.porgcoat.2006.01.002)
14. Barszczewska-Rybarek I (2012) Quantitative determination of degree of conversion in photocured poly(urethane-dimethacrylate)s by Fourier transform infrared spectroscopy. *J Appl Polym Sci* 123(3):1604–1611. doi:[10.1002/app.34553](https://doi.org/10.1002/app.34553)
15. Litvinov VM, Dias AA (2001) Analysis of network structure of UV-cured acrylates by ^1H NMR relaxation, ^{13}C NMR Spectroscopy, and dynamic mechanical experiments. *Macromolecules* 34(12):4051–4060. doi:[10.1021/ma010066u](https://doi.org/10.1021/ma010066u)
16. Rwei SP, Chen JD, Su CM (2013) Kinetics of UV-curing of waterborne polyurethane acrylate dendrimer. *Polym Bull* 70:1019–1035. doi:[10.1007/s00289-012-0868-x](https://doi.org/10.1007/s00289-012-0868-x)
17. Asmussen E, Peutzfeldt A (1998) Influence of UEDMA, BisGMA and TEGDMA on selected mechanical properties of experimental resin composites. *Dent Mater* 14(1):51–56
18. Ferracane J (1985) Correlation between hardness and degree of conversion during the setting reaction of unfilled dental restorative resins. *Dent Mater* 1:11–14

19. Achilias DS, Karabela MM, Sideridou ID (2008) Thermal degradation of light-cured dimethacrylate resins. Part I. Isoconversional kinetic analysis. *Thermochim Acta* 472:74–83. doi:[10.1016/j.tca.2008.02.004](https://doi.org/10.1016/j.tca.2008.02.004)
20. Reddy KR, Raghu AV, Jeong HM, Siddaramaiah (2009) Synthesis and characterization of pyridine-based polyurethanes. *Des Monom Polym* 12:109–118. doi:[10.1163/156855509X412054](https://doi.org/10.1163/156855509X412054)
21. Reddy KR, Raghu AV, Jeong HM (2008) Synthesis and characterization of novel polyurethanes based on 4,4'-[1,4-phenylenebis(methylylidenenitrilo)]diphenol. *Polym Bull* 60:609–616. doi:[10.1007/s00289-008-0896-8](https://doi.org/10.1007/s00289-008-0896-8)
22. Londono JD, Habenschuss A, Curro JG, Rajasekaran JJ (1996) Short-range order in some polymer melts from X-ray diffraction. *J Polym Sci B Polym Phys* 34(17):3055–3061
23. Thakral S, Terban MW, Thakral NK, Suryanarayanan R (2016) Recent advances in the characterization of amorphous pharmaceuticals by X-ray diffractometry. *Adv Drug Deliv Rev* 100:183–193. doi:[10.1016/j.addr.2015.12.013](https://doi.org/10.1016/j.addr.2015.12.013)
24. Barszczewska-Rybarek I, Gibas M, Kurcok M (2000) Evaluation of the network parameter in aliphatic poly(urethane dimethacrylate)s by dynamic thermal analysis. *Polymer* 41:3129–3135
25. Barszczewska-Rybarek I, Korytkowska A, Gibas M (2001) Investigations on the structure of poly(dimethacrylate)s. *Des Monom Polym* 4(4):301–314
26. Barszczewska-Rybarek IM (2013) Prediction of physical properties of dimethacrylate polymer networks by a group contribution approach. *Int J Polym Anal Charact* 18:93–104. doi:[10.1080/1023666X.2013.747286](https://doi.org/10.1080/1023666X.2013.747286)
27. Reiche A, Sandner R, Weinkauff A, Sandner B, Fleischer G, Wittig F (2000) Gel electrolytes on the basis of oligo(ethylene glycol)_n dimethacrylates—thermal, mechanical and electrochemical properties in relationship to the network structure. *Polymer* 41(10):3821–3836